AIP | Applied Physics Letters

Principles of femtosecond X-ray/optical cross-correlation with X-ray induced transient optical reflectivity in solids

S. Eckert, M. Beye, A. Pietzsch, W. Quevedo, M. Hantschmann, M. Ochmann, M. Ross, M. P. Minitti, J. J. Turner, S. P. Moeller, W. F. Schlotter, G. L. Dakovski, M. Khalil, N. Huse, and A. Föhlisch

Citation: Applied Physics Letters **106**, 061104 (2015); doi: 10.1063/1.4907949
View online: http://dx.doi.org/10.1063/1.4907949
View Table of Contents: http://scitation.aip.org/content/aip/journal/apl/106/6?ver=pdfcov
Published by the AIP Publishing

Principles of femtosecond X-ray/optical cross-correlation with X-ray induced transient optical reflectivity in solids

S. Eckert,[1,a)] M. Beye,[1,a)] A. Pietzsch,[1] W. Quevedo,[1] M. Hantschmann,[1] M. Ochmann,[2] M. Ross,[3] M. P. Minitti,[4] J. J. Turner,[4] S. P. Moeller,[4] W. F. Schlotter,[4] G. L. Dakovski,[4] M. Khalil,[3] N. Huse,[2] and A. Föhlisch[1,5]

[1]*Institute for Methods and Instrumentation in Synchrotron Radiation Research, Helmholtz-Zentrum Berlin für Materialien und Energie GmbH, Albert-Einstein-Str. 15, 12489 Berlin, Germany*
[2]*Institute for Nanostructure and Solid State Physics, University of Hamburg, Jungiusstr. 11, 20355 Hamburg, Germany and Max Planck Institute for the Structure and Dynamics of Matter, Center for Free-Electron Laser Science, Luruper Chaussee 149, 22761 Hamburg, Germany*
[3]*Department of Chemistry, University of Washington, Box 351700, Seattle, Washington 98195, USA*
[4]*LCLS, SLAC National Accelerator Laboratory, 2575 Sand Hill Road, Menlo Park, California 94025, USA*
[5]*Institut für Physik und Astronomie, Universität Potsdam, Karl-Liebknecht-Str. 24/25, 14476 Potsdam, Germany*

(Received 20 January 2015; accepted 30 January 2015; published online 10 February 2015)

The discovery of ultrafast X-ray induced optical reflectivity changes enabled the development of X-ray/optical cross correlation techniques at X-ray free electron lasers worldwide. We have now linked through experiment and theory the fundamental excitation and relaxation steps with the transient optical properties in finite solid samples. Therefore, we gain a thorough interpretation and an optimized detection scheme of X-ray induced changes to the refractive index and the X-ray/optical cross correlation response. © *2015 AIP Publishing LLC*. [http://dx.doi.org/10.1063/1.4907949]

Ultrafast X-ray induced optical reflectivity changes are used at X-ray free-electron lasers worldwide as a powerful tool for femtosecond X-ray/optical cross-correlation.[1–5,26,27] This method is essential to enable scientific research, for example, in the fields of phase transition dynamics,[6,7,28] and of photo-catalysis and chemistry.[8,9,29] X-ray/optical cross correlation has produced rich and sometimes seemingly contradictory behavior depending on the experimental conditions regarding X-ray and optical wavelength, excitation densities, as well as sample material and detection geometries. In order to exploit the full potential of this approach, it is crucial to predict and quantitatively describe the fundamental physics of X-ray induced modifications in a given sample probed in optical reflectivity measurements.

In this work, we introduce a conceptual model in direct relation to experimental findings for the ultrafast dynamics of the refractive index of solids after intense X-ray irradiation. We gain a consistent description of the transient optical properties of solids under intense femtosecond X-ray excitation. Due to its favorable material properties, silicon nitride (Si_3N_4) has been chosen as sample material in an optimized detection geometry.

The response of the material to the X-ray irradiation evolves on different time scales.

First, core excited states result from the absorption of X-ray photons in a sample. Choosing the X-ray photon energy close to core level resonances yields high absorption cross sections and hence increased excitation densities. Soft X-ray (SXR) excitation at the nitrogen K-shell absorption resonance creating core-excitations in silicon nitride will be considered. More than 99% of the nitrogen core excited states decay via the emission of high energy auger electrons within the core hole lifetime of 5 fs.[10,11] Their high kinetic energy is transformed to valence excitations at other lattice sites in a scattering cascade within the excited sample. The deposited energy of the X-ray pump pulse is thus converted at early timescales into low-energy electron-hole pairs across the band gap.[12]

Second, energy is transferred from the electronic to the phonon system through electron-phonon coupling. The heat capacities of electrons and the lattice determine the equilibrated temperature which is reached within picoseconds after the excitation in this two temperature model.[13]

The optical response of an excited sample depends on both the initial electronic excitation[14] and the following picosecond dynamics of the hot lattice.[15] The optical reflectivity as a function of material, incidence angle, and film thickness is given by an extension of the Fresnel formula dependent on the complex refractive index of layers within the sample and the used probe wavelength.[16] We therefore study the transient modifications of the complex refractive index $\tilde{n}$ in a sample which depends on the optical probe wavelength λ and a given excitation density ρ,

$$\tilde{n}(\rho,\lambda) = [n(\lambda) + \Delta n(\rho,\lambda)] + i[k(\lambda) + \Delta k(\rho,\lambda)].$$

The changes of the refractive index and hence the reflectivity of X-ray excited insulators can be related to the dynamics described above.[17] Within the first picosecond after the excitation, hot, mobile carriers in the sample alter the refractive index through Drude-like free carrier absorption. Additionally, band filling effects result in altered optical absorption cross sections for inter- and intraband transitions while correlation effects between the inserted carriers induce a shrinkage of the band gap in the insulator.

Within the first picosecond after the excitation, the lattice is also substantially heated through electron-phonon coupling. Thermal band gap shrinkage (-3.7×10^{-4} eV/K for Si_3N_4[18]) alters the index on longer timescales.

[a)]Authors to whom correspondence should be addressed. Electronic addresses: sebastian.eckert@helmholtz-berlin.de and martin.beye@helmholtz-berlin.de.

By studying the reflectivity of a supported thin film sample, we can analyze the impact of these dynamics on changes of the complex index of refraction. The low absorption for probe photon energies below the band gap of the sample material [$k(\lambda) = 0$ and disregarding band tail absorption] enables long path lengths of radiation within thin film insulating samples. Interference between radiation which is reflected at the two interfaces of the thin sample layer with a thickness d can be exploited to highlight changes of the real part of the refractive index. We focus on λ dependent reflectivity minima for p-polarized probe radiation shown in Figure 1 where the reflectivity as a function of incidence angle and layer thickness is given. The minima occur for a wide range of incidence angles and optical path lengths of odd multiples of $\lambda/2$ within the film and at the Brewster angle (64° for Si_3N_4). Choosing the optimized geometry at these minima yields high sensitivity to changes in the real part of the refractive index and overall enhanced relative changes in reflectivity.

Experimentally, we reach an optimized geometry at a reflectivity minimum within our 185 nm Si_3N_4 film on a silicon substrate at 20° angle of incidence utilizing 470 nm radiation (Figure 1(b) square). Poor detection conditions are created under identical geometry using 400 nm probe radiation (Figure 1(a) circle).

The reflectivity changes were induced by unmonochromatized X-ray pulses originating from 120 fs (FWHM) short electron bunches with photon energies at the nitrogen 1s absorption resonance at the SXR materials beam line of the LCLS in Stanford.[19] The experiments were conducted on the time tool in the liquid jet endstation (LJE).[20] The deposited energy density within the silicon nitride layer ranges from 1.5 to 4.8 kJ/cm^3.[21] The optical 470 nm and 400 nm probe pulses had p-polarization with 50 fs (FWHM) duration.

The resulting X-ray induced relative optical reflectivity changes of the sample are presented for the poor and the optimized geometry and X-ray excitation below and above (solid and empty markers) the nitrogen 1s absorption threshold within the Si_3N_4 film in Figures 2(b) and 2(c), respectively. We observe a 5 fold increased contrast in the optimized detection geometry.

The temporal evolution of the reflectivity changes can be separated in two domains. Short lived reflectivity changes are present within the first 500 fs after the excitation of the sample. They decay into a metastable state with an altered

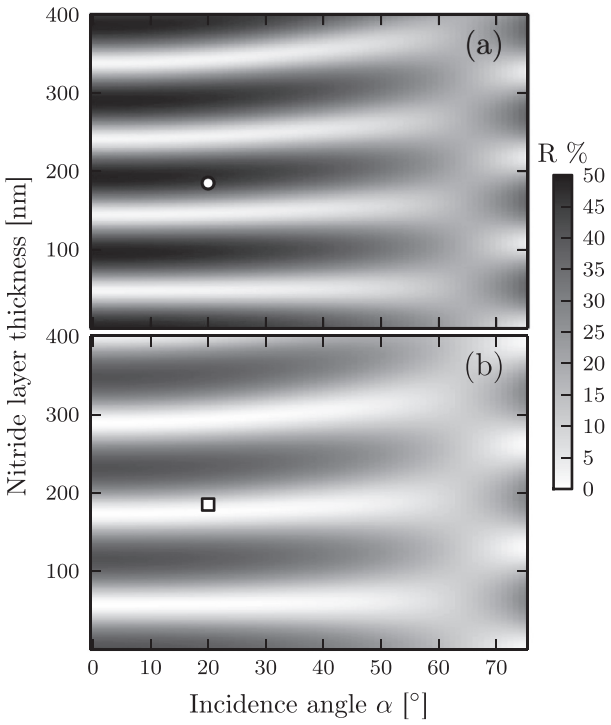

FIG. 1. Optical reflectivity of a Si_3N_4 film on a silicon substrate. The detection geometry reaches optimized at reflectivity minima at the Brewster angle of 64° and at incidence angles with optical path length of odd multiples of $\lambda/2$ within the Si_3N_4 film. Detection geometry at 20° incidence angle and a 185 nm Si_3N_4 film are marked for (a) $\lambda = 400$ nm, resulting in a reflectivity maximum, and (b) $\lambda = 470$ nm, resulting in a reflectivity minimum.

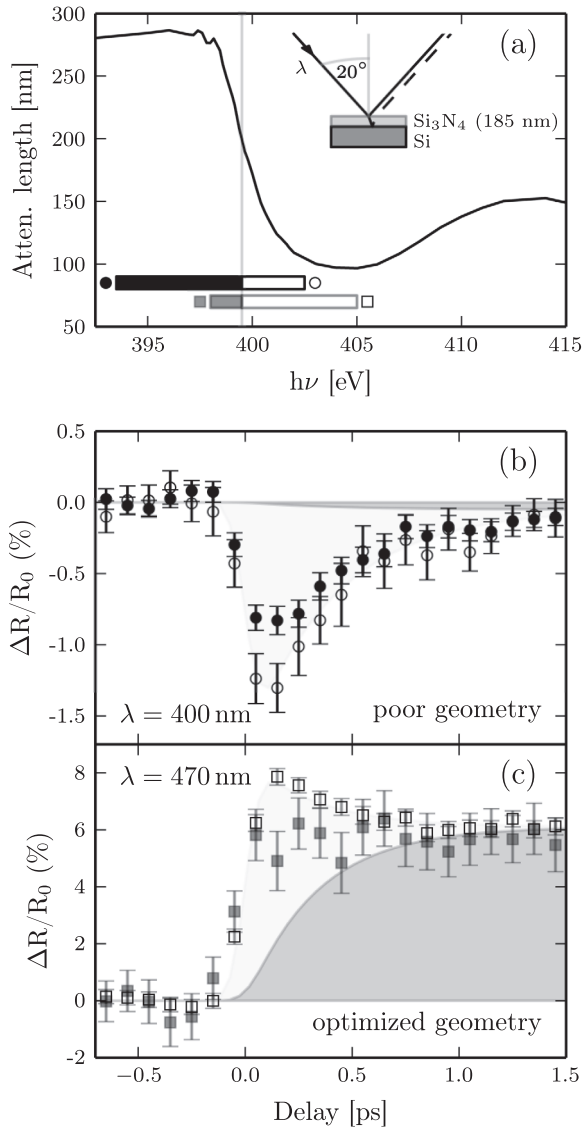

FIG. 2. Role of the experimental configuration in measurements of relative reflectivity changes $\Delta R/R_0$. (a) X-ray attenuation length in silicon nitride for photon energies at the nitrogen K-edge. Bars with associated markers indicate bin ranges for the data in (b) and (c) and in Figure 3. The inset illustrates the experimental geometry. (b) The poor geometry yields relative reflectivity changes up to (1.3 ± 0.2)%. (c) The optimized conditions yield relative reflectivity changes up to (7.9 ± 0.3)%. Short and long lived features are indicated by grey regions. Those are correlated with the equilibration between initially excited electrons and the lattice.

reflectivity and a lifetime much longer than the probed picosecond timescale. For optimized conditions, both the long and short lived reflectivity changes are pronounced in Figure 2(c). For the poor detection geometry at a probe wavelength of 400 nm in Figure 2(b), the short lived component is pronounced while the long lived part is absent. The short lived features increase in amplitude for higher incidence photon energies (see Figure 2). We correlate the short lived features in the reflectivity measurements with both the altered real and imaginary parts of the refractive index in the silicon nitride layer [$\Delta n(\rho, \lambda) \neq 0$, $\Delta k(\rho, \lambda) > 0$], and we conclude that the long lived component is dominated by real index changes [$\Delta n(\rho, \lambda) > 0$] which we probe with high selectivity in the optimized geometry. Similar behavior of the complex refractive index at high excitation densities has been reported recently by Casolari *et al.*[22]

Let us link the detected evolution of the complex refractive index with the dynamics within the excited Si_3N_4 layer. The initial exclusively electronic excitation causes changes of both the real and the imaginary parts of the refractive index. Energy transfer by electron phonon scattering on longer timescales yields a temperature increase in the excited layer of 1.6×10^3 K at an excitation density of 3.9 kJ/cm^3 in the performed experiment.[23] An X-ray attenuation length of 135 nm for photon energies above the nitrogen absorption edge is assumed. The resulting band gap shrinkage theoretically causes an increase of the real part of the refractive index in the Si_3N_4 layer on the order of 10^{-2}, modeling the long lived reflectivity changes in Figure 2(c). Note that band gap shrinkage is the only process inducing an index increase for probe photon energies below the band gap of the sample.[14]

For this reason, Si_3N_4 with 4.5 eV band gap[24,25] is a very well suited material. Both the long and short lived reflectivity changes are strong in an optimized experimental geometry. In contrast to that metallic samples lack the long-timescale component.[5] The absence of a band gap leads to the absence of a long-lived reflectivity change related to band gap shrinkage through thermal heating.[15]

Now we turn to the dependence on the exciting X-ray fluence. The excitation density within the sample has been altered by changing the X-ray energy across the nitrogen absorption edge. The corresponding effective excitation depth is illustrated in Figure 3(a).

Short temporal as well as long lived components of the reflectivity change saturate as the effective excitation depth is on the order of the nitride layer thickness. The phase shift and the total attenuation of the optical wave which is transmitted through the nitride layer are proportional to the integral change of the refractive index in the probed volume. Hence, the detected reflectivity change is dependent on the total pulse energy only as long as the nitride layer thickness exceeds the attenuation length of the pump photons.

Summarizing the correlation between the presented effects one should take the following aspects into account to optimize the detection efficiency of X-ray induced refractive index changes in layered samples. The insulating sample material should feature a high absorption cross section for the X-ray pump photon energy used. The dominant process causing the change of the refractive index strongly depends on the band structure of the sample. The probe photon energy should be chosen as close to the band gap as possible where bandfilling and band gap shrinkage effects peak.[14] The reflectivity should be minimized exploiting interference effects that depend on the probe wavelength, the refractive indices of the sample, the layer thickness, and the angle of incidence. A universal applicability can be gained by choosing the nitride layer thickness larger than the attenuation length of the X-ray photons used for the excitation.

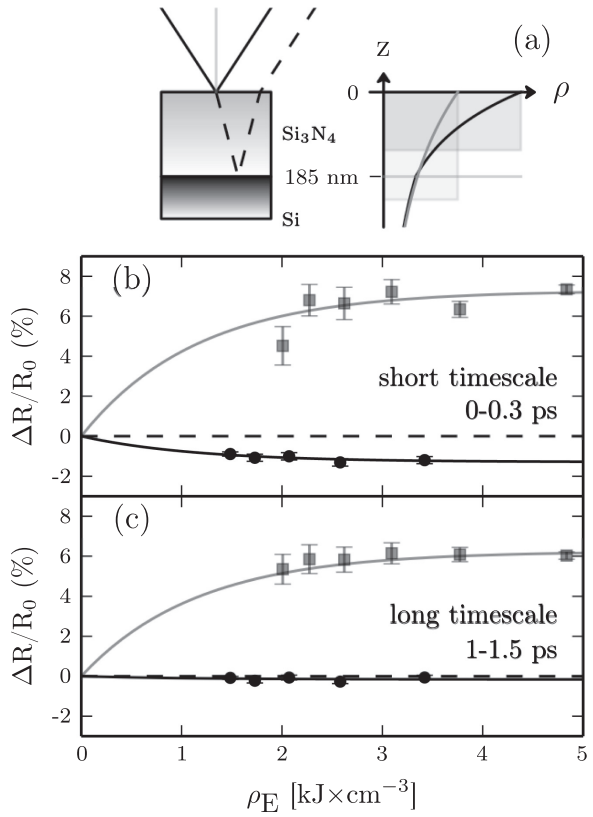

FIG. 3. X-ray pump excitation density dependence of the X-ray/optical cross-correlation $\Delta R/R_0$ for optimized and poor detection geometry. (a) Schematic illustration of the depth dependent excitation density ρ for strong and weak absorption yielding effective excitation depths (grey) below and above the nitride layer thickness. Reflectivity changes on short (b) and long timescales (c). Saturation occurs for attenuation lengths below the nitride layer thickness, whereas the optimized geometry yields a much higher total reflectivity change. Markers indicate the probe wavelength. Saturation functions have been fitted to the data to guide the eye.

We demonstrated the adjustable selectivity for the detection of altered refractive indices induced by X-rays in a thin silicon nitride layer. The dynamics in X-ray excited insulating materials on ultrashort timescales and correlated reflectivity changes were interpreted by taking the purely electronic excitation and the subsequent coupling to the lattice into account. Additionally, we presented an optimized experimental layout for the detection of X-ray induced changes of a material's refractive index in the context of X-ray/optical cross correlation.

This research was carried out on the SXR Instrument at the Linac Coherent Light Source (LCLS) at the SLAC National Accelerator Laboratory. The SXR Instrument is funded by a consortium whose membership include the LCLS, Stanford University through the Stanford Institute for Materials and Energy Sciences (SIMES), Lawrence Berkeley

National Laboratory (LBNL), University of Hamburg through the BMBF priority program FSP 301, and the Center for Free Electron Laser Science (CFEL). The LCLS is funded by the DOE Office of Basic Energy Sciences. We gratefully acknowledge the support of the LCLS staff. This work was supported by the Volkswagen Stiftung. The financial support of the Helmholtz-Virtual-Institute VI 419 "Dynamic Pathways in Multidimensional Landscapes" was thankfully acknowledged. M.R. and M.K. acknowledge support from the Office of Basic Energy Sciences of the U.S. Department of Energy Grant No. DE-SC0002190 and the David and Lucille Packard Foundation. We thank Hana Cho for support during the measurement of the absorption spectrum of the silicon nitride membrane and Christian Weniger for the sample preparation.

[1]C. Gahl, A. Azima, M. Beye, M. Deppe, K. Döbrich, U. Hasslinger, F. Hennies, A. Melnikov, M. Nagasono, A. Pietzsch *et al.*, Nat. Photonics **2**, 165 (2008).
[2]T. Maltezopoulos, S. Cunovic, M. Wieland, M. Beye, A. Azima, H. Redlin, M. Krikunova, R. Kalms, U. Frühling, F. Budzyn *et al.*, New J. Phys. **10**, 033026 (2008).
[3]M. Beye, O. Krupin, G. Hays, A. Reid, D. Rupp, S. de Jong, S. Lee, W.-S. Lee, Y.-D. Chuang, R. Coffee *et al.*, Appl. Phys. Lett. **100**, 121108 (2012).
[4]M. R. Bionta, N. Hartmann, M. Weaver, D. French, D. Nicholson, J. Cryan, J. Glownia, K. Baker, C. Bostedt, M. Chollet *et al.*, Rev. Sci. Instrum. **85**, 083116 (2014).
[5]O. Krupin, M. Trigo, W. Schlotter, M. Beye, F. Sorgenfrei, J. Turner, D. Reis, N. Gerken, S. Lee, W. Lee *et al.*, Opt. Express **20**, 11396 (2012).
[6]N. Pontius, T. Kachel, C. Schüßler-Langeheine, W. Schlotter, M. Beye, F. Sorgenfrei, C. Chang, A. Föhlisch, W. Wurth, P. Metcalf *et al.*, Appl. Phys. Lett. **98**, 182504 (2011).
[7]M. Beye, F. Sorgenfrei, W. F. Schlotter, W. Wurth, and A. Föhlisch, Proc. Natl. Acad. Sci. U. S. A. **107**, 16772 (2010).
[8]M. Dell'Angela, T. Anniyev, M. Beye, R. Coffee, A. Föhlisch, J. Gladh, T. Katayama, S. Kaya, O. Krupin, J. LaRue *et al.*, Science **339**, 1302 (2013).
[9]M. Beye and A. Föhlisch, Chem. Phys. **414**, 130 (2013).
[10]M. O. Krause, J. Phys. Chem. Ref. Data **8**, 307 (1979).
[11]M. Neeb, J.-E. Rubensson, M. Biermann, and W. Eberhardt, J. Electron Spectrosc. Relat. Phenom. **67**, 261 (1994).
[12]N. Medvedev, B. Ziaja, M. Cammarata, M. Harmand, and S. Toleikis, Contrib. Plasma Phys. **53**, 347 (2013).
[13]O. Osmani, N. Medvedev, M. Schleberger, and B. Rethfeld, Phys. Rev. B **84**, 214105 (2011).
[14]B. R. Bennett, R. A. Soref, and J. A. del Alamo, IEEE J. Quantum Electron. **26**, 113 (1990).
[15]S.-S. Wellershoff, J. Hohlfeld, J. Güdde, and E. Matthias, Appl. Phys. A **69**, S99 (1999).
[16]B. Harbecke, Appl. Phys. B **39**, 165 (1986).
[17]S. M. Durbin, AIP Adv. **2**, 042151 (2012).
[18]J. Bauer, Phys. Status Solidi A **39**, 411 (1977).
[19]W. Schlotter, J. Turner, M. Rowen, P. Heimann, M. Holmes, O. Krupin, M. Messerschmidt, S. Moeller, J. Krzywinski, R. Soufli *et al.*, Rev. Sci. Instrum. **83**, 043107 (2012).
[20]K. Kunnus, I. Rajkovic, S. Schreck, W. Quevedo, S. Eckert, M. Beye, E. Suljoti, C. Weniger, C. Kalus, S. Grübel *et al.*, Rev. Sci. Instrum. **83**, 123109 (2012).
[21]K. Tiedtke, A. Sorokin, U. Jastrow, P. Juranić, S. Kreis, N. Gerken, M. Richter, U. Arp, Y. Feng, D. Nordlund *et al.*, Opt. Express **22**, 21214 (2014).
[22]F. Casolari, F. Bencivenga, F. Capotondi, E. Giangrisostomi, M. Manfredda, R. Mincigrucci, E. Pedersoli, E. Principi, C. Masciovecchio, and M. Kiskinova, Appl. Phys. Lett. **104**, 191104 (2014).
[23]J. F. Shackelford and W. Alexander, *CRC Materials Science and Engineering Handbook* (CRC Press, 2010).
[24]H. R. Philipp, J. Electrochem. Soc. **120**, 295 (1973).
[25]A. Shaposhnikov, I. Petrov, V. Gritsenko, and C. Kim, Phys. Solid State **49**, 1628 (2007).
[26]M. Harmand, R. Coffee, M. R. Bionta, M. Chollet, D. French, D. Zhu, D. M. Fritz, H. T. Lemke, N. Medvedev, B. Ziaja *et al.*, "Achieving few-femtosecond time-sorting at hard X-ray free-electron lasers," Nature Photonics **7**, 215–218 (2013).
[27]N. Hartmann, W. Helml, A. Galler, M. R. Bionta, J. Grünert, S. L. Molodtsov, K. R. Ferguson, S. Schorb, M. L. Swiggers, S. Carron *et al.*, "Sub-femtosecond precision measurement of relative X-ray arrival time for free-electron lasers," Nature Photonics **8**, 706–709 (2014).
[28]Y. D. Chuang, W. S. Lee, Y. F. Kung, A. P. Sorini, B. Moritz, R. G. Moore, L. Patthey, M. Trigo, D. H. Lu, P. S. Kirchmann *et al.*, "Real-time manifestation of strongly coupled spin and charge order parameters in stripe-ordered nickelates via time-resolved resonant x-ray diffraction," Phys. Rev. Lett. **110**, 127404 (2013).
[29]K. R. Siefermann, C. D. Pemmaraju, S. Neppl, A. Shavorskiy, A. A. Cordones, J. Vura-Weis, D. S. Slaughter, F. P. Sturm, F. Weise, H. Bluhm *et al.*, "Atomic Scale Perspective of Ultrafast Charge Transfer at a Dye-Semiconductor Interface," J. Phys. Chem. Lett. **5**, 2753 (2014).